

Rapid distortion theory for differential diffusion

P. R. Jackson,¹ C. R. Rehmann,² J. A. Sáenz,³ and H. Hanazaki⁴

Received 24 February 2005; revised 21 March 2005; accepted 18 April 2005; published 17 May 2005.

[1] Rapid distortion theory (RDT) is used to examine differential diffusion of active and passive scalars in unshered, initially isotropic turbulence. RDT is well suited to study differential diffusion because it applies to strongly stratified flows with weak turbulence—that is, the conditions under which differential diffusion occurs. The theory reproduces several key features of the evolution of scalar fluxes and scalar flux spectra observed in direct numerical simulations (DNS). Predictions of the diffusivity ratio match laboratory results well when a parameter of the theory is related to a parameter of the experiments. RDT also allows parameters such as molecular diffusivities to be varied over a wider range than DNS can currently reach. RDT may prove to be a useful tool for computing mixing in weakly turbulent parts of the stratified ocean interior and possibly for parameterizing subgrid scale mixing in general circulation models. **Citation:** Jackson, P. R., C. R. Rehmann, J. A. Sáenz, and H. Hanazaki (2005), Rapid distortion theory for differential diffusion, *Geophys. Res. Lett.*, 32, L10601, doi:10.1029/2005GL022443.

1. Introduction

[2] The large difference between the molecular diffusivities of temperature and salinity can lead to differential diffusion, or preferential transport of temperature in a fluid with double-diffusively stable profiles of temperature and salinity. Differential diffusion is important for several problems in oceanography, including the interpretation of vertical mixing and ocean modeling [Gargett, 2003]. Laboratory experiments show that differential diffusion occurs for $\epsilon/\nu N^2$ less than $O(10^3)$, where ϵ is the rate of dissipation of turbulent kinetic energy, ν is the kinematic viscosity, and N is the buoyancy frequency [Jackson and Rehmann, 2003]. Such values are typical of ocean interior regions away from the surface and rough boundaries, including the main and upper equatorial thermoclines, the polar pycnocline, and the abyssal ocean and near abyssal slopes [Moum, 1997]. In fact, field measurements near the Oregon coast suggest that differential diffusion does occur in the ocean [Nash and Moum, 2002].

[3] Direct numerical simulations have provided information on the mechanisms leading to differential diffusion.

Resolution requirements are stringent because simulations must resolve the velocity and scalar fields and the molecular diffusivities D_T and D_S of temperature and salinity are small: The Schmidt numbers $Sc_T = \nu/D_T$ and $Sc_S = \nu/D_S$ are 7 and 700, respectively. To model a heat-salt system, Merryfield *et al.* [1998] simulated two-dimensional flows; initial conditions mimicked turbulent bursts caused by wave breaking. Differential diffusion was largest for strong stratification and weak turbulence, and the maximum difference between the temperature and salt fluxes occurred when they switched from downgradient to upgradient. To represent the turbulence more accurately, Gargett *et al.* [2003] studied three-dimensional flows with $\tau = D_S/D_T = 0.1$. By examining cospectra of the vertical velocity and scalar (or flux spectra), they suggested that preferential transport of the high-diffusivity scalar requires larger upgradient fluxes of the low-diffusivity scalar at high wavenumbers. By comparing the simulations of two- and three-dimensional flows, Gargett *et al.* [2003] argued that the results for $\tau = 0.1$ provide a lower bound for differential diffusion in the oceanic case of $\tau = 0.01$.

[4] To isolate processes responsible for upgradient fluxes and study a range of parameters, we model differential diffusion with rapid distortion theory (RDT). Several features of RDT make it suitable for studying this problem. For a stratified flow, RDT applies to weak turbulence in strong stratification, or under the conditions when differential diffusion occurs. Also, RDT predicts upgradient fluxes and flux spectra that have upgradient flux at high wavenumbers when the Schmidt number is large [Hanazaki and Hunt, 1996]. Furthermore, although RDT is an approximate theory, a larger range of parameters, especially Schmidt number, can be studied. After describing the assumptions behind RDT, we demonstrate the usefulness of RDT for studying and predicting differential diffusion.

2. Rapid Distortion Theory

[5] In RDT, products of fluctuations in the equations for fluctuating momentum and buoyancy are neglected. As a consequence, no energy cascade develops, and the evolution of the turbulence is determined by interactions between eddies and the mean flow or stratification. RDT was originally applied to flows with strong strain or strong shear [e.g., Townsend, 1980]. For stratified flow, Hanazaki and Hunt [1996] compared the nonlinear term in the momentum equation to the buoyancy term and concluded that RDT applies to eddies of size λ and larger if the Froude number $Fr_\lambda = u_\lambda/N\lambda$ is small.

[6] Rapid distortion theory works with the equations for fluctuating momentum, temperature, and salinity. We consider homogeneous turbulence subjected to linear, stable temperature and salinity profiles and zero mean velocity.

¹Department of Civil and Environmental Engineering, University of Illinois at Urbana-Champaign, Urbana, Illinois, USA.

²Department of Civil, Construction, and Environmental Engineering, Iowa State University, Ames, Iowa, USA.

³Department of Theoretical and Applied Mechanics, University of Illinois at Urbana-Champaign, Urbana, Illinois, USA.

⁴Department of Mechanical Engineering, Kyoto University, Yoshida-Honmachi, Sakyo-ku, Kyoto, Japan.

Following *Hanazaki and Hunt* [1996], the RDT equations for the vertical velocity, temperature, and salinity are

$$\frac{d\hat{u}_3}{dt'} = \left[\frac{\kappa_3^2}{\kappa^2} - 1 \right] (\hat{u}_S - \hat{u}_T) - Gr^{-1} \kappa^2 \hat{u}_3, \quad (1a)$$

$$\frac{d\hat{u}_T}{dt'} = -\frac{R_\rho}{R_\rho + 1} \hat{u}_3 - (GrSc_T)^{-1} \kappa^2 \hat{u}_T, \quad (1b)$$

$$\frac{d\hat{u}_S}{dt'} = \frac{1}{R_\rho + 1} \hat{u}_3 - (GrSc_S)^{-1} \kappa^2 \hat{u}_S, \quad (1c)$$

where hats denote Fourier coefficients, $t' = Nt$, $N^2 = g(\alpha d\bar{T}/dx_3 - \beta d\bar{S}/dx_3)$ is the squared buoyancy frequency, α and β are the coefficients of thermal expansion and haline contraction, x_3 is the vertical coordinate, $\hat{u}_T = g\alpha\hat{T}/N$, and $\hat{u}_S = g\beta\hat{S}/N$. The dimensionless wavenumber is $\kappa = k\mathcal{L}$, and the length scale \mathcal{L} is related to the longitudinal integral scale ℓ by $\mathcal{L} = (\pi/2)^{-1/2} \ell$ [Townsend, 1980]. The dimensionless parameters are the Schmidt numbers, the density ratio $R_\rho = -(\alpha d\bar{T}/dx_3)/(\beta d\bar{S}/dx_3)$, and the Grashof number $Gr = N\mathcal{L}^2/\nu$, which measures the relative importance of buoyancy and viscous forces.

[7] Scalar fluxes are computed by deriving and solving equations for the spectra E_{ij} . For example, methods of *Hanazaki and Hunt* [1996] give the equation for the cospectrum of vertical velocity and temperature as

$$\frac{dE_{T3}}{dt'} = \left[\frac{\kappa_3^2}{\kappa^2} - 1 \right] (E_{TS} - E_{TT}) - \frac{R_\rho}{R_\rho + 1} E_{33} - Gr^{-1} (1 + Sc_T^{-1}) \kappa^2 E_{T3}. \quad (2)$$

We impose zero initial temperature and salinity fluctuations and an initially isotropic velocity field, which has the energy spectrum (normalized by $q_0^2 \mathcal{L}^3$)

$$E_{ij}(\underline{\kappa}, 0) = \frac{E(\kappa)}{4\pi\kappa^2} \left(\delta_{ij} - \frac{\kappa_i \kappa_j}{\kappa^2} \right), \quad (3)$$

where the normalized energy spectrum function $E(\kappa) = 1/(3\sqrt{2\pi}) \kappa^4 e^{-\frac{1}{2}\kappa^2}$ is appropriate for the final period of decay, in which nonlinear transfer is small [Hanazaki and Hunt, 1996]. The equations for the spectra are then solved numerically. Several tests were done to ensure adequate resolution in time and wavenumber space.

[8] After the flux spectra are integrated over all wavenumbers to compute the fluxes $F_T = -\overline{u'_T u'_3}$ and $F_S = \overline{u'_S u'_3}$, the fluxes are integrated in time and used to quantify differential diffusion in terms of the diffusivity ratio $d = R_\rho [\int_0^\infty F_S dt / \int_0^\infty F_T dt]$, or the ratio of the eddy diffusivities of salt and heat. In practice, we integrated the fluxes over 38 buoyancy periods ($240 N^{-1}$), or the approximate time between stirring periods in the experiments of *Jackson and Rehmann* [2003].

3. Results and Discussion

[9] RDT reproduces several qualitative features in the evolution of the vertical scalar fluxes seen in the DNS of *Merryfield et al.* [1998] and *Gargett et al.* [2003]. Initially,

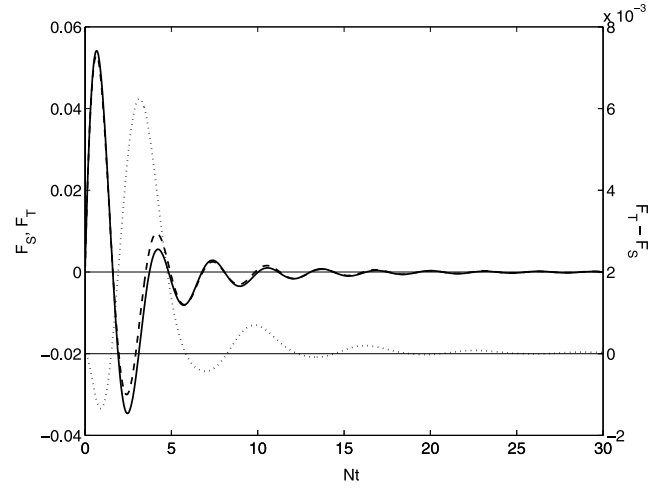


Figure 1. Evolution of scalar fluxes for $Gr = 10$. The solid line represents salt flux F_S , the dashed line represents heat flux F_T , and the dotted line is $F_T - F_S$. Positive fluxes are downgradient. For clarity the origin for the flux difference is shifted below the origin for the fluxes.

the salinity flux and the temperature flux are both downgradient (Figure 1), and the flux of the lower diffusivity scalar (salt) exceeds the flux of the higher diffusivity scalar (temperature). After a quarter buoyancy period, the fluxes switch to upgradient, and the lower diffusivity scalar experiences more upgradient flux than the higher diffusivity scalar. The fluxes oscillate between downgradient and upgradient with a period of π/N . RDT shows that the fluxes are nearly equal over most of the evolution with small differences near the extrema that lead to differential diffusion. Also, RDT predicts that the flux difference switches sign just before the fluxes switch from upgradient to downgradient and that the maximum flux difference occurs slightly before the end of the first restratification phase. *Gargett et al.* [2003] reported similar observations from their DNS.

[10] The evolution of scalar flux spectra computed with RDT resembles the spectral evolution sketched by *Gargett et al.* [2003] in several ways. Initially, both spectra are downgradient with a greater downgradient flux of salt (Figure 2a). As the turbulence decays, the fluxes switch to upgradient at the high wavenumbers first (Figure 2b) and then progressively become upgradient for all wavenumbers (Figure 2c). As in the DNS, the flux spectra for both scalars become upgradient at the same wavenumber, and the upgradient flux of the low diffusivity scalar exceeds that of the high diffusivity scalar. The flux spectra oscillate between downgradient and upgradient, as the evolution of the fluxes, which are the integrals of the spectra, would suggest (Figure 1). The amplitude of oscillation decreases with time, and the amplitude decreases faster for lower Gr . The largest contribution to differential diffusion comes from the excess upgradient fluxes of salt in the first period of upgradient flux (Figures 1 and 2c).

[11] Our application of RDT does not capture the difference in the wavenumber ranges of the flux spectra computed with DNS. Because RDT does not allow an energy cascade to develop, the maximum wavenumber range remains the same as that set by the initial conditions, or in our case the

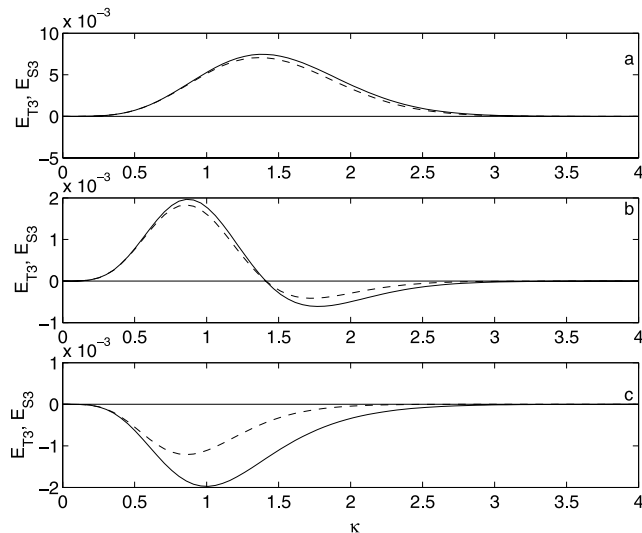


Figure 2. Evolution of nondimensional vertical scalar flux spectra for $Gr = 1$. (a) $Nt = 0.37$; (b) $Nt = 1.11$; (c) $Nt = 2.73$. The solid line is E_{S3} and the dashed line is E_{T3} .

initial energy spectrum function $E(\kappa)$. However, in DNS, because of the difference in Batchelor wavenumbers, flux spectra of a low diffusivity scalar develop larger wavenumber ranges than flux spectra of a high diffusivity scalar [Gargett *et al.*, 2003]. Differences in the spectral values accompanied differences in the wavenumber range, and Gargett *et al.* [2003] attributed differential diffusion to excess upgradient fluxes at high wavenumbers. As shown below, our calculations suggest differential diffusion can occur even when the wavenumber ranges for the two flux spectra are the same. Using initial scalar spectra with different wavenumber ranges would yield spectra that resemble those from DNS more closely, and differential transport should increase.

[12] RDT reproduces laboratory observations of differential diffusion. Curves of diffusivity ratio as a function of Gr for several values of τ and Sc are shown in Figure 3 with the measurements of Jackson and Rehmann [2003] and J. E. Martin and C. R. Rehmann (Layering in a flow with diffusively stable temperature and salinity stratification, submitted to *Journal of Physical Oceanography*, 2004, hereinafter referred to as Martin and Rehmann, submitted manuscript, 2004); the results of Jackson and Rehmann [2003] were recomputed with the method of Martin and Rehmann (submitted manuscript, 2004), which allows the eddy diffusivities to vary with vertical position. Varying the density ratio does not change the diffusivity ratio significantly, as Jackson and Rehmann [2003] found. For example, the diffusivity ratios for $R_\rho = 0.5$ and 1 differ by less than 2% over the entire range in Figure 3, and they differ by less than 0.5% over the Grashof number range corresponding to the experiments. Also, RDT predicts $d = 1$ for large Gr and a decrease in the diffusivity ratio as Gr decreases (Figure 3). The predicted curve follows a similar trend to the laboratory measurements, which are expressed as a function of $\epsilon/\nu N^2$. In fact, the theory and the measurements agree well if

$$Gr = 7\epsilon/\nu N^2. \quad (4)$$

The agreement is good for both the less energetic flows for which RDT should work well and the more energetic flows to which RDT does not strictly apply.

[13] The relationship between the parameter of the experiments and the parameter of the theory is reasonable. The inertial estimate for dissipation $\epsilon \sim u^3/\ell$ can be used in equation (4) to obtain a Froude number based on integral scales of 0.45, which is consistent with the condition for RDT to apply. Also, equation (4) would hold if $\ell \approx 3.3 L_O$, where $L_O = (\epsilon/N^3)^{1/2}$ is the Ozmidov scale. The Ozmidov scale becomes relevant in strongly stratified flows. For example, *Itsweire et al.* [1986] argued that the onset of buoyancy effects, defined as the departure of the Ellison scale L_t from passive-scalar behavior, occurs when $L_t = 0.85 L_O$. The larger coefficient required for (4) to hold for our calculations indicates even stronger stratification effects, as expected for a model based on small time scales for gravitational adjustment. In fact, the Ellison scale exceeds the Ozmidov scale late in the evolution of several of the runs of *Itsweire et al.* [1986].

[14] Our application of RDT predicts that the diffusivity ratio approaches unity for large Grashof numbers. In the laboratory measurements of Jackson and Rehmann [2003], values of d slightly greater than 1 occurred at high $\epsilon/\nu N^2$. Such values would seem possible if the excess downgradient salt flux in the initial mixing phase (e.g., Figure 2a) exceeds the excess upgradient salt flux in the restratification phase (e.g., Figure 2b). In fact, in our calculations, the

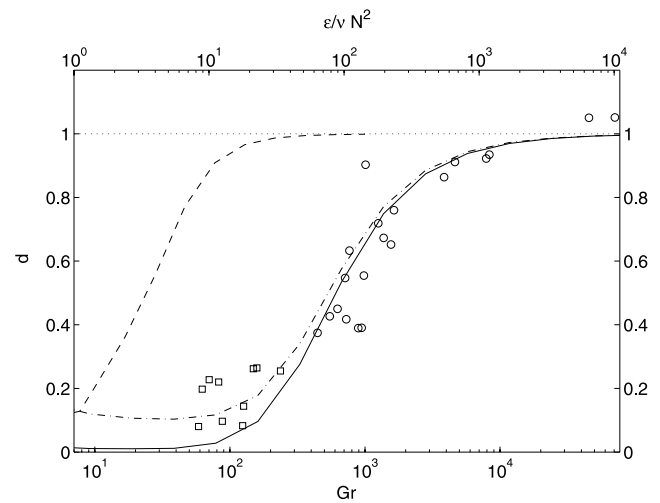


Figure 3. Diffusivity ratio as a function of the Grashof number predicted with RDT (solid and dashed lines, lower abscissa) and as a function of $\epsilon/\nu N^2$ for laboratory observations (symbols, upper abscissa). The solid line is RDT for $Sc_T = 7$ and $Sc_S = 700$, the dot-dash line is RDT for $Sc_T = 7$ and $Sc_S = 70$, and the dashed line is RDT for passive dyes with $Sc_T \approx 2300$ and $Sc_S \approx 21,000$ in a salt stratification. In the cases that do not correspond to temperature and salinity, Sc_T is the Schmidt number for the high-diffusivity scalar, and Sc_S is the Schmidt number for the low-diffusivity scalar. All RDT calculations with active scalars had $R_\rho = 1$. The open circles are the reprocessed data of Jackson and Rehmann [2003], and the open squares come from the experiments of Martin and Rehmann (submitted manuscript, 2004).

diffusivity ratio exceeded unity only for very small Grashof numbers (not shown), at which the system was damped heavily enough that restratification was insignificant. Different initial conditions with initial scalar spectra that extend over different wavenumber ranges may allow RDT to predict $d > 1$ for large Grashof number.

[15] A key feature of RDT is its ability to model scalars with small molecular diffusivities, like that for saltwater. We considered two cases aside from the salt-heat case in equations (1a)–(1c). The first uses passive dyes with $Sc \approx 2300$ and $Sc \approx 21,000$ in a salt stratification, as in the breaking internal wave experiments of *Hebert and Ruddick* [2003]. RDT captures the trend in the diffusivity ratio and predicts differential diffusion will occur at lower Gr (or $\epsilon/\nu N^2$) (Figure 3). The latter result is qualitatively consistent with results of *Hebert and Ruddick* [2003], but they found differential diffusion to become important at $\epsilon/\nu N^2 = O(0.1)$, or two orders of magnitude smaller than what RDT predicts for homogeneous turbulence. This shift could be due to several factors. One is the relation between the Grashof number and $\epsilon/\nu N^2$. Another is the difference in the mechanisms generating the turbulence: We imposed homogeneous, initially isotropic turbulence on a stratified flow, but a breaking internal wave likely evolves much differently.

[16] A case with Schmidt numbers of 7 and 70 was considered to determine how the diffusivity ratio depends on τ . In evaluating the relevance of their three-dimensional simulations with $\tau = 0.1$ for the oceanic case of a heat-salt system ($\tau = 0.01$), *Gargett et al.* [2003] compared two-dimensional simulations with $\tau = 0.1$ and $\tau = 0.01$ [*Merryfield et al.*, 1998]. Differential diffusion was 20–40% smaller for $\tau = 0.1$ than for $\tau = 0.01$, and the two-dimensional flows had more differential diffusion than three-dimensional flows, possibly because of differences in the energy cascades. *Gargett et al.* [2003] concluded that their DNS at $\tau = 0.1$ provides a lower bound on differential diffusion within 40%. RDT also predicts that the $\tau = 0.1$ case has less differential diffusion (i.e., larger d) than the $\tau = 0.01$ case (Figure 3). The two cases are within 10% for $Gr > 600$ and within 40% for $Gr > 300$. However, at low Grashof number (or $\epsilon/\nu N^2$), when d is small, the $\tau = 0.1$ case greatly underpredicts the amount of differential diffusion that occurs in the oceanic case.

[17] We recommend using RDT to study the physics of differential diffusion and incorporating it into subgrid scale models of weakly turbulent, strongly stratified parts of the ocean interior. For strongly stratified flows RDT is physically more appealing than models that use a gradient-transport approach, including models with specified eddy diffusivities and two-equation turbulence models. Gradient-transport models apply to flows in which the

timescale of the turbulence is small compared to the timescale of the mean flow, or high Froude number in stratified flow, while RDT is suited to model the strongly stratified, weakly turbulent flows in which differential diffusion occurs. Also, although some of the more sophisticated models based on the Reynolds-averaged Navier-Stokes (RANS) equations can reproduce upgradient flux, eddy diffusivity and two-equation models, which are commonly used in ocean modeling, cannot. Furthermore, no RANS model can predict the wavenumber dependence of upgradient fluxes that *Gargett et al.* [2003] argued was crucial for differential diffusion. Because relatively little computational effort is required in RDT, it can model heat, salt, dyes, chemical tracers, and arbitrary scalars more easily than DNS can. This feature makes RDT attractive for exploring the physics of differential diffusion and interpreting studies of mixing in strongly stratified flows.

[18] **Acknowledgment.** This work was supported by the National Science Foundation under grant OCE 99-77208 and an NDSEG Fellowship to P. R. Jackson.

References

- Gargett, A. E. (2003), Differential diffusion: An oceanographic primer, *Prog. Oceanogr.*, *56*, 559–570.
- Gargett, A. E., W. J. Merryfield, and G. Holloway (2003), Direct numerical simulation of differential scalar diffusion in three-dimensional stratified turbulence, *J. Phys. Oceanogr.*, *33*, 1758–1782.
- Hanazaki, H., and J. C. R. Hunt (1996), Linear processes in unsteady stably stratified turbulence, *J. Fluid Mech.*, *318*, 303–337.
- Hebert, D., and B. R. Ruddick (2003), Differential mixing by breaking internal waves, *Geophys. Res. Lett.*, *30*(2), 1042, doi:10.1029/2002GL016250.
- Itsweire, E. C., K. N. Helland, and C. W. Van Atta (1986), The evolution of grid-generated turbulence in a stably stratified fluid, *J. Fluid Mech.*, *162*, 299–338.
- Jackson, P. R., and C. R. Rehmann (2003), Laboratory measurements of differential diffusion in a diffusively stable, turbulent flow, *J. Phys. Oceanogr.*, *33*, 1592–1603.
- Merryfield, W. J., G. Holloway, and A. E. Gargett (1998), Differential vertical transport of heat and salt by weak stratified turbulence, *Geophys. Res. Lett.*, *25*, 2773–2776.
- Moum, J. N. (1997), Quantifying vertical fluxes from turbulence in the ocean, *Oceanography*, *10*, 111–115.
- Nash, J. D., and J. N. Moum (2002), Microstructure estimates of turbulent salinity flux and the dissipation spectrum of salinity, *J. Phys. Oceanogr.*, *32*, 2312–2333.
- Townsend, A. A. (1980), *The Structure of Turbulent Shear Flow*, Cambridge Univ. Press, New York.

H. Hanazaki, Department of Mechanical Engineering, Kyoto University, Yoshida-Honmachi, Sakyo-ku, Kyoto 606-8501, Japan.

P. R. Jackson, Department of Civil and Environmental Engineering, University of Illinois at Urbana-Champaign, Urbana, IL 61801, USA.

C. R. Rehmann, Department of Civil, Construction, and Environmental Engineering, Iowa State University, Ames, IA 50011, USA. (rehmann@iastate.edu)

J. A. Sáenz, Department of Theoretical and Applied Mechanics, University of Illinois at Urbana-Champaign, Urbana, IL 61801, USA.